© 2014. Published by The Company of Biologists Ltd | Development (2014) 141, 1894-1905 doi:10.1242/dev.099333

RESEARCH ARTICLE

Arabidopsis UNHINGED encodes a VPS51 homolog and reveals a role for the GARP complex in leaf shape and vein patterning

Shankar Pahari, Ryan D. Cormark, Michael T. Blackshaw, Chen Liu, Jessica L. Erickson and Elizabeth A. Schultz*

ABSTRACT

Asymmetric localization of PIN proteins controls directionality of auxin transport and many aspects of plant development. Directionality of PIN1 within the marginal epidermis and the presumptive veins of developing leaf primordia is crucial for establishing leaf vein pattern. One mechanism that controls PIN protein distribution within the cell membranes is endocytosis and subsequent transport to the vacuole for degradation. The *Arabidopsis* mutant *unhinged-1* (*unh-1*) has simpler leaf venation with distal non-meeting of the secondary veins and fewer higher order veins, a narrower leaf with prominent serrations, and reduced root and shoot growth. We identify *UNH* as the *Arabidopsis* vacuolar protein sorting 51 (VPS51) homolog, a member of the *Arabidopsis* Golgi-associated retrograde protein (GARP) complex, and show that UNH interacts with VPS52, another member of the complex and colocalizes with trans Golgi network and pre-vacuolar complex markers. The GARP complex in yeast and metazoans retrieves vacuolar sorting receptors to the trans-Golgi network and is important in sorting proteins for lysosomal degradation. We show that vacuolar targeting is reduced in *unh-1*. In the epidermal cells of *unh-1* leaf margins, PIN1 expression is expanded. The *unh-1* leaf phenotype is partially suppressed by *pin1* and *cuc2-3* mutations, supporting the idea that the phenotype results from expanded PIN1 expression in the marginal epidermis. Our results suggest that UNH is important for reducing expression of PIN1 within margin cells, possibly by targeting PIN1 to the lytic vacuole.

KEY WORDS: Leaf vein patterning, Leaf shape, PIN1 localization, GARP, Retrograde trafficking, VPS51

INTRODUCTION

The reticulate leaf vein pattern typical of dicotyledonous plants such as *Arabidopsis* is formed progressively during leaf development (Berleth and Mattsson, 2000; Berleth et al., 2000; Scarpella et al., 2004; Steynen and Schultz, 2003). The auxin signal flow canalization hypothesis (Sachs, 1981) predicts that auxin distribution narrows from a wide field of cells to a subset of cells with high auxin transport that then become the sites for vasculature. Polar transport capacity is due to asymmetric distribution of PIN FORMED1 (PIN1) protein, the auxin efflux carrier (Steinmann et al., 1999), the expression of which in developing veins mirrors the pattern of auxin distribution predicted by the canalization model (Scarpella et al., 2006; Wenzel et al., 2007).

In developing leaves, PIN1 expression in the epidermal cells of the leaf margin predicts the position of PIN expression domains (PEDs) that narrow to form veins (Scarpella et al., 2006). Initially, PIN1 localization is apical within epidermal cells of the young leaf primordium, directing an auxin maximum at the distal tip (Benkova et al., 2003; Reinhardt et al., 2003). The distal auxin maximum induces an initially wide PED in internal primordial cells that narrows to a file of cells with basal PIN1 localization, predicting the formation of the midvein (Bayer et al., 2009; Hou et al., 2010; Scarpella et al., 2006; Wenzel et al., 2007). Concurrently, PIN1 polarity in the distal marginal epidermal cells shifts from apical to basal, establishing lateral auxin maxima within the marginal epidermis (marginal epidermal PED, MEPED) on either side of the leaf. The process of shifting PIN1 polarity within the marginal epidermis, disappearance of distal MEPEDs and emergence of more proximal MEPEDs repeats during leaf formation. Successive MEPEDs are associated with: (1) margin outgrowth and the formation of serrations; and (2) PIN1 expression in the adjacent ground meristem that predicts the position of the secondary veins (Bilsborough et al., 2011; Scarpella et al., 2006; Wabnik et al., 2010; Wenzel et al., 2007). During secondary vein formation, two domains form sequentially: (1) the lower loop domain (LLD), which extends from the lateral convergence point to the proximal midvein; and (2) the upper loop domain (ULD), which extends from the LLD to the distal midvein (Scarpella et al., 2006; Wabnik et al., 2010; Wenzel et al., 2007). Failure to form a complete ULD is observed in mutants that show a disconnected vein network (Hou et al., 2010).

Dynamic relocalization of PIN1 proteins in both epidermal and ground meristem is crucial in establishing vascular fate and vein pattern (Dhonukshe et al., 2007; Geldner et al., 2003). Localization of PIN proteins is dependent upon vesicle cycling. PIN proteins at the plasma membrane (PM) undergo clathrin-dependent endocytosis to the early endosome/TGN. Post-TGN trafficking of endocytosed PIN involves either recycling or degradative pathways. Recycling back to the plasma membrane is mediated by GNOM, a guanine-nucleotide exchange factor for ADP-ribosylation factor GTPases: ARF-GTPases. The role of GNOM in polarized PIN1 localization within leaves is supported by the observation that *gnom* mutants show defects to leaf vein patterning (Koizumi et al., 2005). A second route carries PIN from early endosomes to the lytic vacuole through late endosomes also known as multi-vesicular bodies (MVBs) or pre-vacuolar complexes (PVCs) (Kleine-Vehn et al., 2008; Laxmi et al., 2008; Oliviusson et al., 2006; Spitzer et al., 2009). Mutation in genes encoding endosomal sorting complex required for transport (ESCRTs) proteins (Spitzer et al., 2009), adaptor protein 3 (AP3) subunits (Feraru et al., 2010) and vacuolar morphology 3 (VAM3) (Shirakawa et al., 2009), which are all orthologs of lysosomal targeting factors in other eukaryotes, result in defects to the localization of PIN protein in the plasma membrane that are often accompanied by its ectopic accumulation within the cytoplasm. The mutations cause defects to various developmental processes, indicating an important regulatory role for vacuolar targeting of PIN.

Department of Biological Sciences, University of Lethbridge, Lethbridge, AB TIK 3M4, Canada.

*Author for correspondence (schultz@uleth.ca)

Received 22 May 2013; Accepted 2 March 2014

Development (2014) 141, 1894-1905 doi:10.1242/dev.099333

The Golgi-associated retrograde protein (GARP) complex is a tetrameric tethering complex consisting of vacuolar protein sorting 51 (VPS51), VPS52, VPS53 and VPS54 subunits. In yeast (Conibear et al., 2003; Reggiori et al., 2003; Siniossoglou and Pelham, 2002), humans (Perez-Victoria et al., 2010a, 2008) and *C. elegans* (Luo et al., 2011), this complex tethers late endosome-derived vesicles at the TGN, allowing retrieval of lysosomal/vacuolar cargo receptors and processing enzymes. Defects to GARP components affect the sorting of lysosomal proteins and maintenance of lysosome function, and result in developmental defects in mice and *C. elegans* (Luo et al., 2011; Schmitt-John et al., 2005). The GARP complex is evolutionarily conserved and present in all eukaryotes (Koumandou et al., 2007). Phenotypes resulting from mutation to three subunits (VPS52, VPS53 and VPS54) of the GARP complex in *Arabidopsis* (Guermonprez et al., 2008; Lee et al., 2006; Lobstein et al., 2004; Wang et al., 2011) suggest that, as in metazoans, the GARP complex has an important developmental role in plants.

The identity and role of the fourth subunit of the plant GARP complex is not yet known. Here, we identify an *Arabidopsis unhinged-1* (*unh-1*) mutant with an open and simplified vein pattern. We show that UNHINGED (UNH) is a VPS51 homolog in *Arabidopsis* and interacts with VPS52, indicating that UNH/VPS51 is part of the GARP complex. Consistent with a role in retrograde trafficking between the late endosome and TGN, we demonstrate that UNH colocalizes with TGN and PVC markers. Supporting a requirement for UNH in vacuolar trafficking, we observe secretion of a vacuolar targeted fluorophore in *unh-1* mutants. *unh-1* leaves have expanded MEPEDs and the *unh-1* phenotype is partially suppressed by mutation of PIN1, suggesting that the phenotype may result from expanded PIN1 expression. Moreover, when exposed to Brefeldin A, PIN1-GFP aggregates into smaller compartments in *unh-1*, suggesting defective PIN1 trafficking. Based on the conserved role of the GARP complex and its importance in targeting proteins for degradation, we suggest that the PIN1 expansion within leaf marginal epidermal cells may be due to improper targeting of PIN1 to the lytic vacuole.

RESULTS

UNH is required for leaf shape and vein pattern

Screening of an EMS mutagenized *Arabidopsis thaliana* (Col-0 background) population for vein patterning defects (Steynen and Schultz, 2003) identified a recessive mutant *unhinged-1* (*unh-1*) [segregation of 3:1 in F2, χ^2=0.55 (P>0.54; n=77)] with fewer secondary and higher order veins and lack of distal vein junctions (Fig. 1B, Table 1). In the first leaves of wild-type plants 21 days after germination (DAG), 5.6% of secondary veins fail to meet distally, whereas in *unh-1* 63% are distally non-meeting (Table 1). In addition, the first leaves in *unh-1* are narrower, as indicated by the length/breadth ratio, and more pointed, and both first and fifth leaves have more prominent serrations than wild type (Table 1, Fig. 1, supplementary material Fig. S1). Like the leaves, *unh-1* cotyledons have a higher number of free-ending veins and thus fewer areoles (Table 2). In addition, *unh-1* plants have shorter primary root length, shorter inflorescence internodes and delayed bolting, but no changes to gravitropic response, root hair length or lateral root density (supplementary material Table S4). The spectrum of defects is consistent with a global defect to the auxin response or auxin transport pathways. To test whether auxin response is affected in *unh-1* plants, we compared expression of the synthetic auxin reporter DR5:GUS (Ulmasov et al., 1997). In both developing leaf lamina and roots, DR5:GUS expression is reduced in *unh-1* compared with wild type, whereas expression in the lateral marginal epidermis at hydathodes appears unchanged at both 16 and 8 h staining times (supplementary material Fig. S2, compare D and E with J and K).

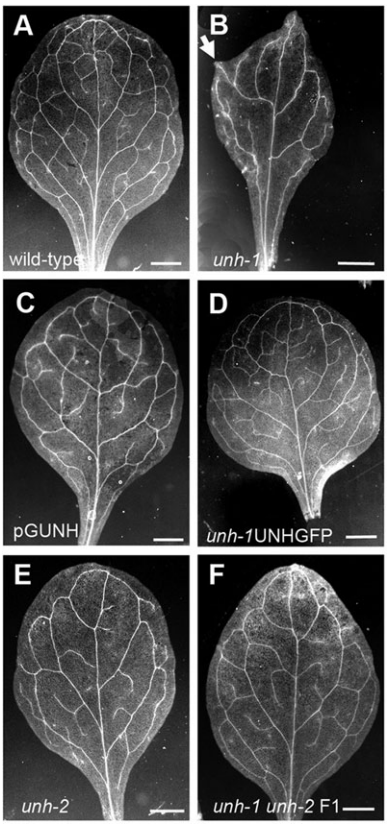

Fig. 1. First leaf phenotype of *unh* alleles and *unh-1* complementation. (A-F) First leaf vein phenotype of 21 DAG: wild type (A), *unh-1* mutant (B),*unh-1* transformed with pGUNH (C), *unh-1* transformed with 35S:UNH-GFP (D), *unh-2* (E) and *unh-1*×*unh-2* F1 (F). Arrow in B indicates serrations. Scale bars: 1 mm.

Map-based cloning of *UNH*

Molecular mapping isolated the *unh-1* mutation to a region between markers 4-11-3 and 4-11-5b on chromosome 4 (supplementary material Fig. S3A-C). Sequencing of candidate genes revealed a G-to-A substitution in the last nucleotide of the 10th intron of the At4g02030.1 gene (supplementary material Fig. S3D), suggesting that a splicing defect may account for the phenotype.

Three experiments confirm that the *unh-1* phenotype is the result of mutation in the At4g02030 gene. First, the *unh-1* phenotype was rescued by introduction of the wild-type At4g02030 gene (pUNH) or 35S:UNH-GFP (Fig. 1C,D). Second, a T-DNA insertion line (GABI_520G08) with an insertion in the 7th intron of At4g02030 (supplementary material Fig. S3D) has significantly reduced tertiary and quaternary veins compared with wild type (Fig. 1E, Table 1) and fails to complement *unh-1* (Fig. 1F, Table 1). We designated GABI_520G08 as *unh-2*. Third, RT-PCR on cDNA from total mRNA using primers flanking the *unh-1* and *unh-2* mutations (arrows in supplementary material Fig. S3D) revealed that the *unh-1* transcript is longer in size and the *unh-2* transcript is lower in intensity compared with the 335 bp wild-type product (supplementary material Fig. S4).

Development (2014) 141, 1894-1905 doi:10.1242/dev.099333

Table 1. Leaf vein pattern and leaf shape characteristics of 21 DAG first leaf and serrations in 28 DAG fifth leaf for various genotypes

Genotype	Number of secondaries	Number of NMS (% of NMS)	Number of tertiaries	Number of quaternaries	Number of areoles	Number of serrations (1st rosette leaves)	First leaf L/B ratio	Number of serrations (5th rosette leaves)
Wild type (52, 30)	8.9±1.4	0.5±0.7 (5.6)	21.3±4.3	4.2±2.2	20.9±4.9	0.1±0.2	1.3±0.1	2.7±1.1
unh-1 (91, 21)	5.7±1.5*	3.6±1.4* (63.1)	5.3±3.1*	0.7±0.8*	3.0±2.5*	0.6±0.8*	1.9±0.5*	5.3±1.1*
unh-2 (19, 17)	8.3±1.1‡	0.8±0.6‡ (9.6)	15.2±3.2*‡	2.6±1.2*‡	15.6±4.1*‡	0.1±0.3‡	1.4±0.1‡	3.5±0.9‡
unh-1×*unh-2* F1 (21, 7)	8.4±0.9‡	0.8±0.7‡ (9.5)	15.9±5.2*‡	2.3±1.6*‡	15.9±4.8*‡	0.2±0.5‡	1.4±0.1‡	3.0±1.0‡
vam3-4 (16, 27)	6.7±1.2*	1.8±1.2*‡ (26.9)	4.8±2.5*	0.6±0.6*	6.1±1.7*	0.4±0.6	1.5±0.1‡	3.7±1.0*‡
unh-1 vam3-4 (21, 19)	3.9±0.8*‡§	3.0±1.1*§ (76.9)	0.3±0.6*‡	0*	1.0±1.1*§	0.4±0.7	2.2±0.9*‡§	5.2±1.0*§
vti11 (18, 21)	9.2±0.6‡	0.8±0.8‡ (8.7)	21.0±4.1‡	3.9±1.9‡	20.8±4.1‡	0.1±0.3‡	1.4±0.1‡	3.8±1.0*‡
unh-1 vti11 (22, 25)	6.3±0.9*§	4.5±1.4*‡§ (71.4)	4.7±2.0*§	0.3±0.5*§	2.1±1.1*§	0.5±0.7*	1.7±0.2*‡	4.7±1.1*
pin1-1 (32, 18)	8.5±1.8‡	0.4±0.7‡ (4.7)	20.9±6.9‡	3.7±3.7‡	20.8±6.3‡	0‡	1.2±0.2‡	0±0*‡
unh-1 pin1-1 (56, 10)	8.9±2.6‡	1.5±1.1*‡§ (16.9)	12.4±8.9*‡§	1.2±1.5*§	11.6±7.3*‡§	0.1±0.4‡	1.5±0.4*‡§	1.6±1.7‡
cuc2-3 (19, 23)	8.8±1.2‡	0.5±0.6‡ (5.7)	24.8±3.2‡	6.7±2.7*‡	24.4±3.4‡	0±0‡	1.3±0.1‡	0±0*‡
unh-1 cuc2-3 (26, 25)	7.3±1.4*‡§	2.7±1.2*‡§ (37.0)	5.5±2.9*§	0.3±0.5*§	4.8±2.4*§	0±0.2‡	1.7±0.2*‡§	0±0*‡
BDLbdl (19, 25)	8.9±1.2‡	0.5±0.5‡ (5.6)	18.4±5.2‡	4.4±2.1‡	17.9±2.9‡	0‡	1.3±0.1‡	3.1±1.0‡
unh-1 BDLbdl (26, 22)	5.0±1.0*§	2.6±1.3*‡§ (52.0)	6.0±2.1*§	0.7±0.7*§	2.5±1.7*§	2.0±0.6*‡§	1.9±0.3*§	7.3±2.4*‡§

Values represent mean±s.d. Numbers in parentheses under 'Genotype' represent number of first leaves scored, number of fifth leaves scored.
NMS, non-meeting secondaries; L/B, leaf length:breadth ratio.
*Significantly different from wild type (ANOVA, Tukey-Kramer test, $P<0.05$).
‡Significantly different from *unh-1* (ANOVA, Tukey-Kramer test, $P<0.05$).
§Double mutant is significantly different from its respective non-*unh-1* single mutant (ANOVA, Tukey-Kramer test, $P<0.05$).

UNH is a member of plant GARP complex

At4G02030/UNH is predicted to encode a VPS51 domain at its N-terminal (Marchler-Bauer et al., 2011) (supplementary material Fig. S3E). The VPS51 protein is one of the four subunits of the GARP complex. UNH contains a well-conserved motif (LVYENYKFISATDT) (supplementary material Fig. S3F) found in the VPS51 domain of higher eukaryotes (Luo et al., 2011) that shares closest homology to *Oryza sativa* and close similarity to *Physcomitrella patens* and *Chlorella variabilis*. Two other genes in *Arabidopsis*, At1g10385 and At5g16300, are also predicted to encode proteins with VPS51 domains but have considerably less conservation of the motif (supplementary material Fig. S3F). SALK lines annotated as having insertions in At5g16300 were screened, but no insertions were detected; observations of lines homozygous for T-DNA insertion in the 4th exon of At1g10385 revealed no obvious phenotype (data not shown), suggesting a less essential role than *UNH*.

Mutations in three subunits (VPS52, VPS53 and VPS54) of the *Arabidopsis* GARP complex have been identified and characterized (Guermonprez et al., 2008; Lobstein et al., 2004; Wang et al., 2011). Insertional mutations in these genes are homozygous lethal and no phenotype similar to *unh-1* has been reported. To determine whether UNH forms part of the GARP complex, we performed yeast two-hybrid assays and tested for interactions between UNH and the other subunits (Kohalmi et al., 1997). Growth in absence of histidine (-His) and synthesis of β-galactosidase indicates that UNH/VPS51 interacts with only VPS52 (supplementary material Fig. S5).

UNH is expressed in both shoot and root

The pleiotropic *unh-1* phenotype suggests that *UNH* acts throughout plant development. The *UNH*-coding region, together with 5 kb upstream, complements the *unh-1* phenotype (Fig. 1C), indicating that the 5 kb region is sufficient to confer the endogenous expression pattern. Thus, we expressed GUS under the 5 kb region (UNH_{prom}:GUS) to assess *UNH* transcription. UNH_{prom}:GUS is expressed in primary roots, lateral roots and shoots of seedlings, as well as in flowers (Fig. 2A-D). In leaves, UNH_{prom}:GUS expression begins weakly and diffusely in 3.5 DAG first leaves, spreads throughout much of the lamina by 4 DAG and becomes increasingly restricted to presumptive veins from 5 to 8 DAG (Fig. 2F-K). Interestingly, UNH_{prom}:GUS is expressed in epidermal cells of the proximal margins (arrows in Fig. 2H,I, magnified in 2J), whereas ATHB8:GUS (Baima et al., 1995; Scarpella et al., 2004) (supplementary material Fig. S2) and FKD1:GUS (Hou et al., 2010), which are expressed similarly within developing veins, are not expressed in leaf margins.

Table 2. Cotyledon vascular phenotype of *unh-1* and wild type

Genotype	Areoles	Veins	Free ending veins
Wild-type (34)	3.3±0.1	3.8±0.1	0.5±0.1
unh-1 (53)	0.9±0.2*	3.9±0.1*	2.0±0.2*

Values represent mean±s.d.
Number in parentheses represents number of cotyledons.
*Significantly different from wild type (Student's *t*-test, $P<0.05$).

UNH colocalizes with both TGN and PVC markers

The *Arabidopsis* VPS52 ortholog POK localizes to post-Golgi compartments (Guermonprez et al., 2008; Lobstein et al., 2004). To determine whether the cellular localization of UNH is consistent with GARP localization in *Arabidopsis* and other organisms, we assessed the localization of UNH-GFP using both stable and transient expression systems. In tobacco epidermal cells, UNH-GFP localizes to small, motile punctate structures (Fig. 3A,D,G,J). UNH-GFP colocalizes frequently (69%, Fig. 3C,P) to the same puncta as RAB5 GTPases Ara7 (RABF2_B; Wave7_Y) and RhaI (RABF2_A; Wave2_Y, data not shown), both of which localize to the PVC (Ebine et al., 2011; Lee et al., 2004). UNH-GFP and SYP61-YFP, a TGN marker (Sanderfoot et al., 2001; Uemura et al., 2004), colocalize to the same structures more frequently (82%, Fig. 3L,P). In yeast, the GARP complex is recruited to the TGN through interaction with yeast protein transport 6 (YPT6) a member of the RAB-GTPase family. In plants, the YPT6 ortholog AtRAB-H1b localizes to the Golgi as well as to smaller, BFA-sensitive compartments, suggesting that AtRAB-H1b may be associated with TGN or endosomal membranes (Johansen et al., 2009). When co-transformed, 93% of UNH-GFP puncta also express YPT6-YFP (Fig. 3I,P). By contrast, 35S:UNH-GFP transiently expressed in tobacco epidermal cells colocalized only rarely with the cis-Golgi marker MEMB12 (Wave127_Y; Fig. 3F,P) (Uemura et al., 2004).

Transformation of 35S:UNH-GFP into *unh-1* plants results in phenotypic reversion to the wild-type phenotype (Fig. 1D),

Development (2014) 141, 1894-1905 doi:10.1242/dev.099333

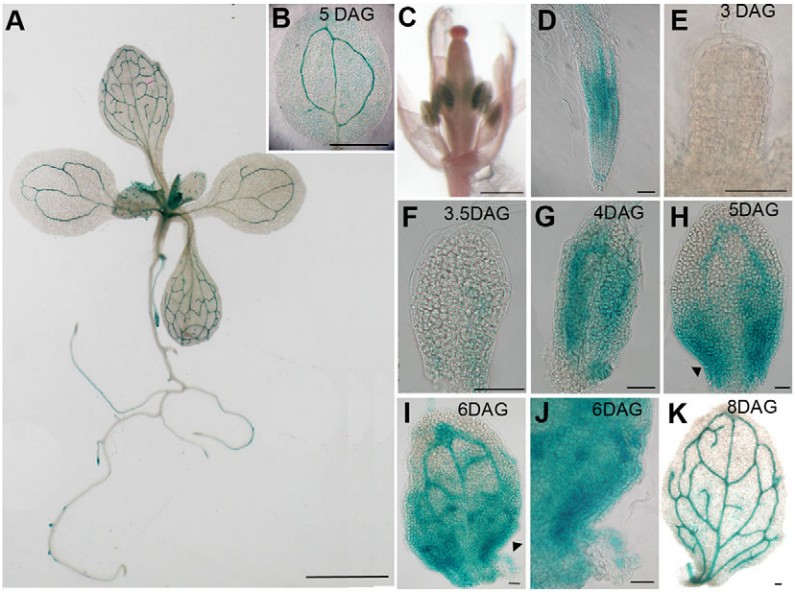

Fig. 2. UNH$_{prom}$:GUS expression in wild type. UNH$_{prom}$:GUS expression in seedling (A), 5 DAG cotyledon (B), floral bud (C), primary root (D) and developing first leaves (E-K). Arrowheads in H and I (region magnified in J) indicate leaf marginal epidermal expression. Scale bars: 1 mm in A; 0.5 mm in B; 50 μm in C-K. All tissues were stained for 24 h, and viewed with a dissecting microscope (A,C) or with a compound microscope with differential interference contrast (B,D-K).

indicating that the fusion protein is fully functional. As when transiently expressed in tobacco, when stably expressed in *Arabidopsis*, UNH-GFP localizes to small, motile punctate structures (Fig. 3M). Because expression is too low for imaging in developing vascular cells, we assessed expression in young cotyledon (5-DAG) epidermal cells, that express UNH$_{prom}$:GUS (Fig. 2B). Introgressing SYP61-YFP into the 35S:UNH-GFP-expressing lines reveals a high level of localization (79%, Fig. 3O,P) to the same punctate structures.

To test whether UNH is involved in PVC/vacuolar pathway, we generated double mutants of *unh-1* with *vam3-4* and *vti11*. Mutations in *VAM3/SYP22*, the product of which is a member of vacuolar membrane-localized t-SNARE superfamily, result in a vein pattern similar to *unh-1* (Shirakawa et al., 2009) (Table 1, Fig. 4C) as well as a shorter shoot (Ohtomo et al., 2005). VTI11, an interacting partner for VAM3, is expressed in the PVC and is a member of the v-SNARE family. *vti11* mutants have a normal leaf vein phenotype (Table 1, Fig. 4E) but enhance *vam3-4* defects (Shirakawa et al., 2009) and have agravitropic shoots (Kato et al., 2002) (supplementary material Fig. S6). Consistent with the genes acting in independent steps to target PIN1 to the vacuole, both *unh-1 vam3-4* and *unh-1 vti11* double mutants show an additive phenotype more extreme than either single mutants with respect to aspects of first leaf vein phenotype (Table 1, Fig. 4D,F) and shoot phenotype (supplementary material Fig. S6).

Vacuolar targeting is disrupted in *unh-1*

Mutation to VPS51 in other eukaryotes has been shown to affect lysosomal structure and mis-sorting of lysosomal cargo to the extracellular space (Luo et al., 2011; Perez-Victoria et al., 2010b; Reggiori et al., 2003). To establish whether *unh-1* causes defects to vacuole structure or targeting, we introduced markers into *unh-1* mutants: VAC-YFP, a tonoplast marker including the C terminus of γ-TIP (Nelson et al., 2007); RHA1-YFP (RABF2A), a marker of PVC (Preuss et al., 2004); and AFVY-RFP, which in wild type is targeted to the lytic vacuole (Hunter et al., 2007). Comparison of VAC-YFP, RHA1-YFP and AFVY-RFP localization and distribution in cotyledon epidermal cells revealed differences between wild-type and *unh-1* (Fig. 5). Whereas RHA1-YFP in wild type is primarily localized to small vesicles of regular size at 5 DAG, the localization in *unh-1* mutants is frequently to larger aggregates of irregular shape and size (Fig. 5A-C). Correspondingly, VAC-YFP identifies primarily large vacuolar bulbs (Saito et al., 2002) in wild type, whereas smaller and more frequent bulbs are seen in *unh-1* (Fig. 5D-F). Finally, we compared localization of AFVY-RFP in wild type and *unh-1*. At early stages of development (3 DAG cotyledons, Fig. 5G,H), AFVY-RFP is within the vacuole in both wild-type and *unh-1* epidermal cells. However, by 6 DAG, localization is strikingly different, being entirely within the vacuole of wild type and entirely secreted to the apoplast in *unh-1* (compare Fig. 5I with 5J). Collectively, these results suggest that, as in other eukaryotes, defects in UNH/VPS51 in *Arabidopsis* affect vacuole structure, disrupt trafficking to the vacuole and result in mis-sorting of vacuolar cargo to the apoplast.

Cellular trafficking is disrupted in *unh-1*

Next, we asked whether *unh-1* is defective in endosome trafficking by using FM4-64, a steryl dye that is incorporated into the plasma membrane and then follows the endocytic pathway to the vacuole (Bolte et al., 2004). Roots of *unh-1* and wild type were treated with FM4-64 for 30 min, rinsed and viewed at hourly intervals. At 1 h, no difference is visible in *unh-1*, suggesting that early endocytic events are not compromised (compare Fig. 6A with 6B). At 3 h, when FM4-64 labels the tonoplast (Dettmer et al., 2006), differences are evident between the two genotypes (compare Fig. 6C with 6D). In both, the tonoplast is labeled, but in *unh-1*, more cellular aggregates are present (Fig. 6E), possibly indicating that the dye is becoming trapped before reaching the vacuole.

The auxin-related defects in *unh-1* mutants combined with the defects to cellular structure and trafficking suggest that *unh-1* may be defective in PIN trafficking. To assess this possibility, we introduced PIN1-GFP and PIN2-GFP into *unh-1*. In roots, localization and intensity of PIN1-GFP and PIN2-GFP in *unh-1* (Fig. 6G,L) are indistinguishable from wild type (Fig. 6F,K). We asked whether *unh-1* might be compromised in PIN2 trafficking by treating with Wortmannin, a PI3 kinase inhibitor that interferes with transport of PIN2 to the vacuole (Kleine-Vehn et al., 2008). Accumulation of PIN2-GFP in root cells of *unh-1* and wild type treated with Wortmannin was not different (Fig. 6J, compare Fig. 6H with 6I), suggesting that *unh-1* may not affect PIN2 trafficking. To test the

Development (2014) 141, 1894-1905 doi:10.1242/dev.099333

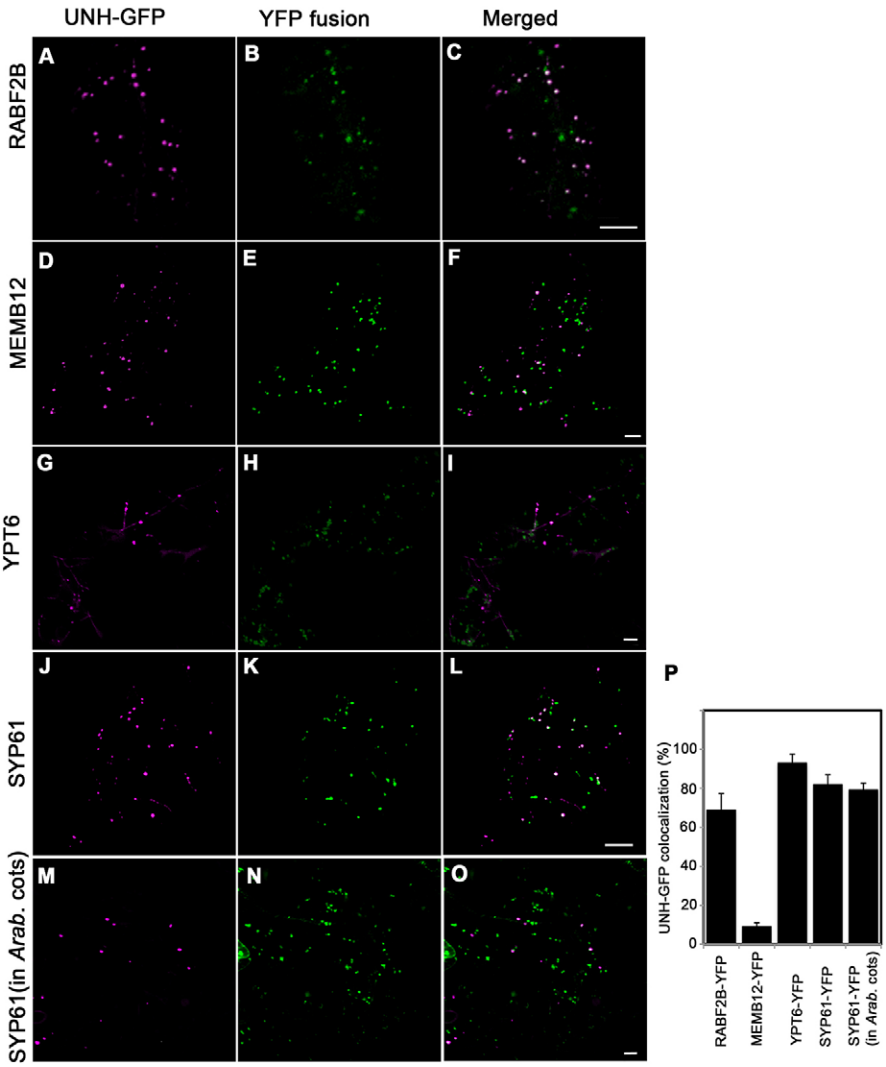

Fig. 3. Colocalization of UNH-GFP. Colocalization of UNH-GFP with PVC (A-C), Golgi (D-F,G-I) and TGN (G-I,J-L,M-O) markers in tobacco (A-L) and *Arabidopsis* (M-O). Confocal images of tobacco leaf cells transiently expressing UNH-GFP (A,D,G,J) and RABF2B-YFP (B), MEMB12-YFP (E), YPT6-YFP (H) or SYP61-YFP (K) with merged expression from both channels in C,F,I,L. Confocal images of a 5 DAG *Arabidopsis* cotyledon cell stably expressing UNH-GFP (M) and SYP61-YFP (N) together with merged image (O). (P) Percentage of UNH-GFP that is colocalized. Data are mean±s.e.m.; *n*=12 (RabF2B), *n*=11 (MEMB12), *n*=15 (YPT6), *n*=11 (SYP61, tobacco) and *n*=31 (SYP61, *Arabidopsis*). Scale bars: 5 μm.

trafficking of PIN1 in *unh-1* mutants, we treated them with Brefeldin A, which interferes with ARF-GEF activity, causing PIN1 endosomes to aggregate into BFA compartments (Geldner et al., 2003). Root cells of *unh-1* mutants treated with BFA formed smaller PIN1-GFP-containing compartments (Fig. 6P, compare Fig. 6M with 6N), suggesting that the identity of the PIN1-containing vesicles is altered and that PIN1 trafficking is compromised in *unh-1* cells.

Expression of PIN1-GFP in epidermal cells of the lateral margin is expanded in *unh-1* leaves

We next examined the PIN1-GFP expression in developing leaves. Our comparison of primordial length and progression of PIN1 expressing domains (PEDs) through vein orders (Table 3) indicates that 2.5 DAG, 3 DAG and 4 DAG wild type are equivalent to developmental stages 3 DAG, 4 DAG and 5 DAG *unh-1* mutants respectively.

PIN1-GFP within epidermal cells at the distal tip (arrows in Fig. 7A,F) and PIN1-GFP within the subepidermal cells along the future midvein vasculature (Fig. 7A,F, Fig. 8) is indistinguishable in *unh-1* and wild type. Concurrent with its expression in the midvein, PIN1-GFP expression at the apical epidermal cells is reduced and new lateral MEPEDs appear. Using an equivalent pixel saturation density as an indication of strong PIN1-GFP expression (see supplementary material Fig. S7), we compared the number of cells showing strong expression of PIN1-GFP within the MEPEDs and their association with the PEDs of secondary veins (Fig. 7, Table 3). These analyses indicate that proximal shifts in MEPEDs and their association with secondary vein formation is similar in *unh-1* and wild type. However, at each stage, the number of cells in MEPEDs is increased in *unh-1* compared with wild type (Table 3, supplementary material Fig. S7) and the level of PIN1-GFP associated with the membrane is often higher in *unh-1* compared with wild type (supplementary material Fig. S7).

PIN1-GFP and ATHB8:GUS expression pattern is altered in *unh-1* secondary veins

unh-1 mutants show defects in serrations and have fewer secondary veins that rarely meet distally (Table 1, Fig. 1B). The MEPEDS generate auxin maxima at the leaf margins that are correlated with both serrations and the generation of secondary veins in leaves (Bilsborough et al., 2011; Scarpella et al., 2010). We asked whether the expanded MEPEDs in *unh-1* are correlated with changes in PIN1-GFP expression in the secondary veins. At early stages, the PED associated with the first secondary vein LLD is indistinguishable between wild type and *unh-1* mutants (Fig. 7B,C,G,H). In 3 DAG wild type, narrowed LLD expression extends to the proximal midvein, whereas ULD expression extends to the distal midvein to form a loop of PIN1 expression that predicts the first set of secondary veins; expression within LLD of the second set of secondary veins is initiated (Fig. 7C). At an equivalent developmental stage of *unh-1*

Development (2014) 141, 1894-1905 doi:10.1242/dev.099333

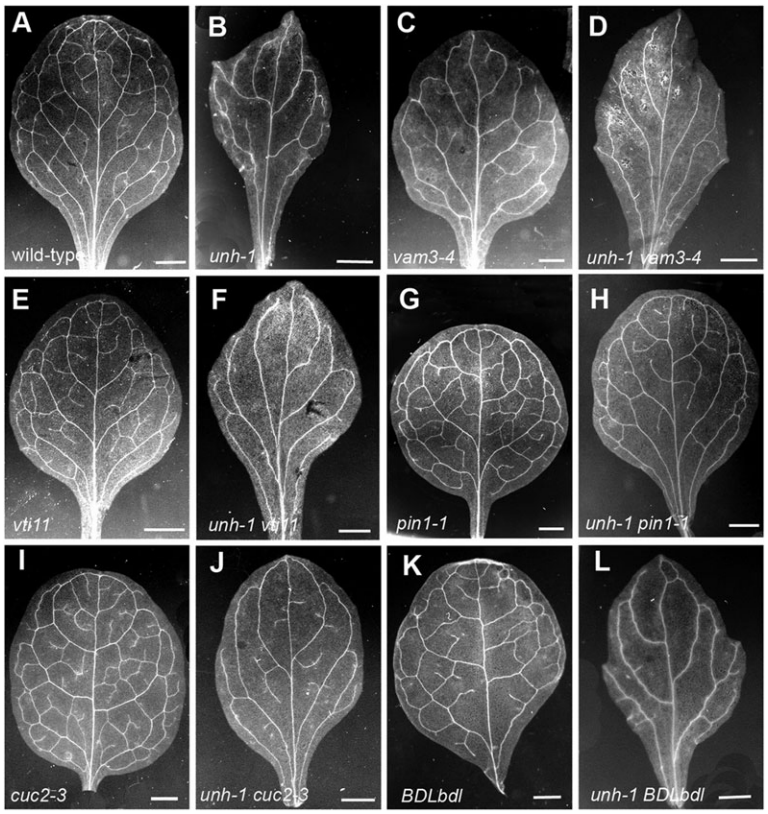

Fig. 4. First leaf phenotype of various genotypes at 21 DAG. Leaf vein phenotype of wild type (A), *unh-1* (B), *vam3-4* (C), *unh-1 vam3-4* (D), *vti11* (E), *unh-1 vti11* (F), *pin1-1* (G), *unh-1 pin1-1* (H), *cuc2-3* (I), *unh-1 cuc2-3* (J), *BDLbdl* (K) and *unh-1 BDLbdl* (L). Scale bars: 1 mm.

(4 DAG), the formation of distal ULD is frequently incomplete (arrowhead in Fig. 7H), a state that persists at later stages (arrowhead in Fig. 7I). Consistent with the PIN1-GFP expression, expression of ATHB8:GUS, a procambial fate marker (Scarpella et al., 2004), is delayed in *unh-1* leaves and does not form complete loops (supplementary material Fig. S2), suggesting that procambial fate fails to be achieved within the distal ULD.

The *unh-1* phenotype is suppressed by *pin1* and *cuc2*, and enhanced by *bdl* mutations

We reasoned that if the *unh-1* leaf phenotype is the result of excess PIN1 expression, it might be rescued by mutation of PIN1. Based on the vein characters we quantified, the *pin1-1* mutant has a first leaf phenotype that is not significantly different from wild type (Table 1, Fig. 4G), whereas the fifth leaf has fewer serrations than wild type (supplementary material Fig. S1). Consistent with our prediction, *pin1-1* reduces the severity of both *unh-1* vein pattern and leaf shape characters, such that the double mutant phenotype is more similar to wild type and significantly different from *unh-1* and *pin1-1* (Table 1, Fig. 4A,B,G,H, supplementary material Fig. S1).

The transcription factor CUC2 acts within the epidermis of the leaf margin to direct PIN1 relocalization and is therefore necessary to generate the epidermal auxin convergence points, and hence auxin response maxima that are correlated with serration and secondary vein development (Bilsborough et al., 2011; Kawamura et al., 2010). Hence, *cuc2-3* mutants fail to develop serrations (Table 1, Fig. 4I, supplementary material Fig. S1). Furthermore, a feedback loop has been proposed such that high auxin response at convergence points negatively regulates CUC2 (Bilsborough et al., 2011). Auxin elicits a transcriptional response through initiating degradation of AUX/IAA transcriptional repressors (such as *BODENLOS*, *BDL*), thereby releasing ARF transcriptional activators (see Quint and Gray, 2006 for a review). Thus, a reduced auxin response is seen in plants heterozygous for a semi-dominant *bdl* allele that encodes a stabilized repressor. Moreover, the reduced auxin response in *BDLbdl* mutants is correlated with elevated CUC2 and an increased number of serrations in fifth leaves (Bilsborough et al., 2011). If aspects of the *unh-1* phenotype results from expanded MEPEDs, we predict that failure to establish PIN1 convergence points (MEPEDs) in a *cuc2-3* mutant would be epistatic to *unh-1* phenotype, whereas the increased CUC2 in a *BDLbdl* mutant might enhance the *unh-1* phenotype.

In support of our hypothesis, absence of *CUC2* in an *unh-1* background eliminates serrations in both first and fifth leaves (Table 1, Fig. 4J, supplementary material Fig. S1). By contrast, the stabilization of BDL in an *unh-1* background increases serration number in *unh-1BDLbdl* first and fifth leaves (Table 1, Fig. 4L, supplementary material Fig. S1). We next asked whether severity of the serration phenotype was correlated with severity of the lamina vein pattern phenotype. The reduced number of serrations in first leaves of the *unh-1 cuc2-3* double mutant is correlated with a suppression of secondary, but not of higher order, vein pattern defects: compared with *unh-1*, the double mutant has increased numbers of secondary veins that meet distally more frequently. By contrast, the increased number of serrations in *unh-1 BDLbdl* is correlated with fewer non-meeting secondary veins (Table 1). The inverse correlation between number of serrations and number of meeting secondary veins strongly suggests that they result from a common defect.

DISCUSSION

UNH is a member of plant GARP complex

Here, we report the identification and characterization of a novel *Arabidopsis* gene, *UNHINGED* (*UNH*), which encodes a homolog of yeast VPS51, the fourth subunit of the tetrameric GARP tethering complex. Previous genomic analyses show high conservation of the VPS51 domain within eukaryotes (Luo et al., 2011). Of the three

Development (2014) 141, 1894-1905 doi:10.1242/dev.099333

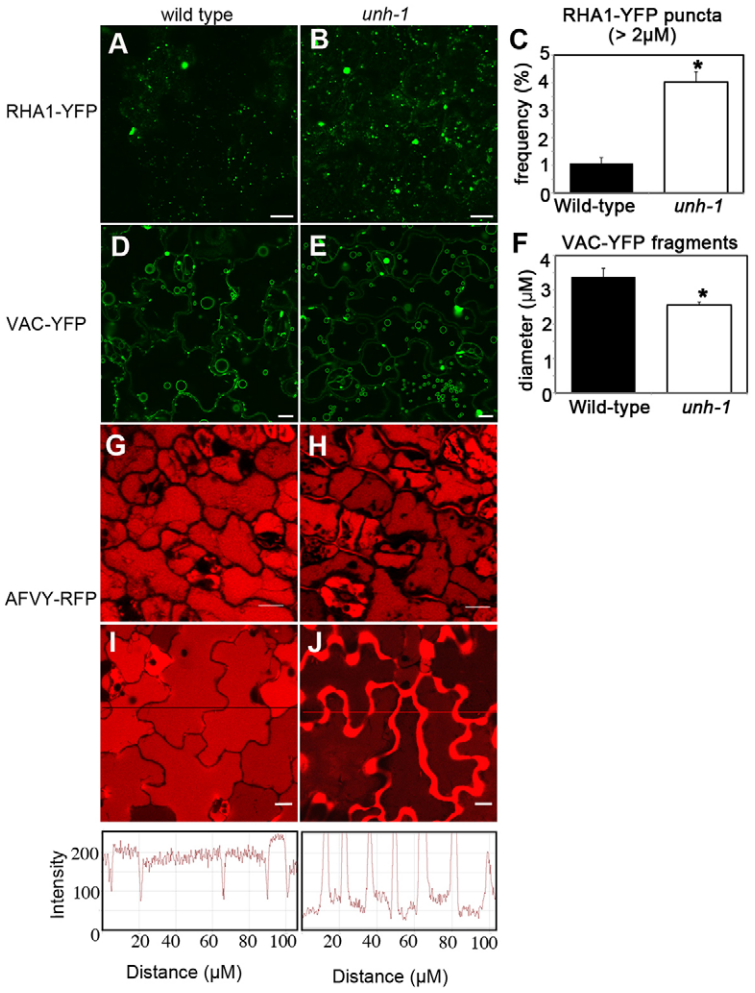

Fig. 5. Cellular phenotype of *unh-1*. Localization of RHA1-YFP (A-C), VAC-YFP (D-F) and AFVY-RFP (G-J) in wild-type and *unh-1* cotyledon epidermal cells at 5 DAG (A,B,D,E), 3 DAG (G,H) and 6 DAG (I,J). (C) The frequency of puncta larger than 2 μm. (F) The diameter of VAC-YFP-labeled fragments. Data are mean±s.e.m., **P*<0.05, Student's *t*-test; *n*=15 (RHA1-YFP; wild type and *unh-1*), *n*=10 (VAC-YFP; wild type and *unh-1*). The horizontal lines in I and J indicate the position at which intensity of RFP emission is measured in the graphs below. Scale bars: 10 μm.

putative VPS51-encoding genes present in *Arabidopsis*, only UNH/VPS51 contains an intact LVYENYNKFISATDT motif (supplementary material Fig. S3) identified as being highly conserved within multicellular eukaryotes (Luo et al., 2011). Our yeast two-hybrid assay shows that UNH/VPS51 interacts with VPS52 (supplementary material Fig. S5). Taken together, these results indicate that UNH is a member of the *Arabidopsis* GARP complex. UNH fails to interact with VPS53 and VPS54, the other two subunits of the complex; similarly, human ANG2 (VPS 51) shows strong interaction with VPS52 and only weak interaction with VPS53 and VPS54 (Perez-Victoria et al., 2010b).

Whereas *unh-1* mutants have a pleiotropic phenotype, our recovery of plants homozygous for either *unh-1* or *unh-2* indicates that these mutations to VPS51 cause neither gametophytic defects nor embryonic lethality. This may suggest that, as in yeast (Conibear et al., 2003), mammals (Perez-Victoria et al., 2010b) and *C. elegans* (Luo et al., 2011), the VPS51 subunit plays an auxiliary role within the GARP complex.

UNH localizes to the TGN and PVC compartments, and mutation causes defects to vacuole targeting

The GARP complex in yeast, humans and *C. elegans* functions in tethering of the LE/PVC-derived lysosomal/vacuolar sorting receptors (VSR) at the TGN, allowing their use in subsequent recognition cycles and in the maintenance of lysosomal function (Conibear et al., 2003; Luo et al., 2011; Perez-Victoria and Bonifacino, 2009; Perez-Victoria et al., 2010b; Reggiori et al., 2003). Our findings that UNH-GFP colocalizes with SYP61 and YPT6, markers of the TGN, as well as RABF2A and RABF2B, markers of the PVC (Fig. 3), support the hypothesis that the GARP complex in plants, as in other eukaryotes, trafficks VSR from the PVC to the TGN. This role is further supported by the defective targeting to the apoplast of the RFP-fused vacuolar-targeting peptide AFVY in *unh-1* mutants (Fig. 5). Similarly, mutation in the mammalian GARP complex blocks the recycling of cation independent mannose-6 phosphate receptor (CIMPR) from the endosome to the TGN, leading to mis-sorting of the CIMPR cargo, lysosomal hydrolases, into the extracellular space (Perez-Victoria et al., 2008). Moreover, *unh-1* mutants differentially localize the endocytic marker FM4-64, alter BFA-induced PIN1-GFP compartments (Fig. 6), form aggregates of RABF2A-localizing compartments and have more fragmented vacuolar compartments identified by VAC-YFP (Fig. 5). Together, these results are consistent with general defects to endomembrane vesicles, vacuole trafficking and maintenance. Structural defects to the lysosome have also been observed in VPS51 mutants in yeast (Reggiori et al., 2003), *C. elegans* (Luo et al., 2011) and mice (Perez-Victoria et al., 2010a), indicating a common role in maintaining vacuolar morphology.

UNH control of PIN1 expression is mediated by PIN1 vacuolar trafficking

During development of the wild-type leaf, distal epidermal convergence points disappear and new, more-proximal, convergence points emerge

Development (2014) 141, 1894-1905 doi:10.1242/dev.099333

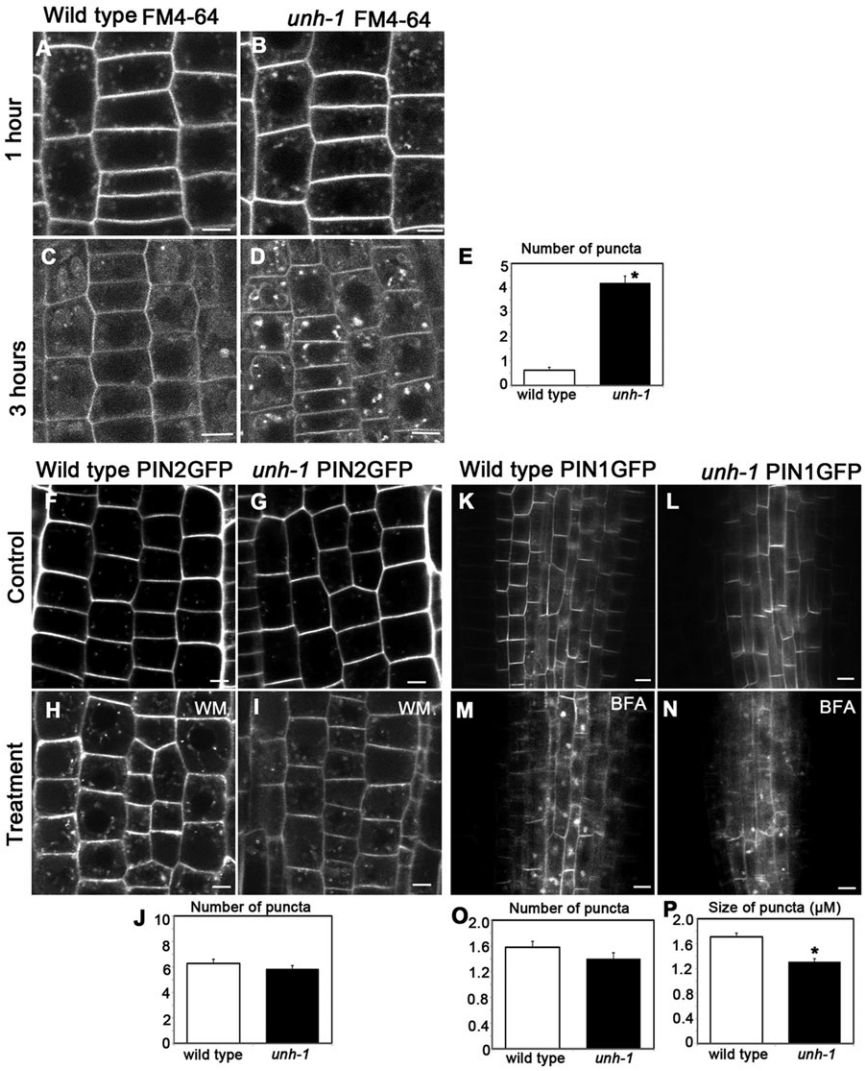

Fig. 6. *unh-1* affects cellular trafficking. Roots of wild type (A,C,F,H,K,M) and *unh-1* (B,D,G,I,L,N). Seedlings treated with 8.2 μM FM4-64 for 30 min were observed after 1 h (A,B) or 3 h (C,D). (E) The frequency of puncta after 3 h. (F-N) Seedlings were treated with 33 μM Wortmannin for 1.5 h (H,I) or with 50 μM BFA for 1.5 h (M,N). (J,O) Frequency of puncta after treatment. (P) Size of puncta after BFA treatment. Data are mean± s.e.m., *P<0.05, Student's t-test; n=60 (FM4-64 wild type and *unh*); n=54 (wortmannin, wild type), n=59, wortmannin, *unh-1*); n=50 (BFA, wild type and *unh-1*). Scale bars: 10 μm.

due to shifting PIN1 expression and localization (Bilsborough et al., 2011; Scarpella et al., 2006). Emergence of each new epidermal convergence point involves an apical-to-basal shift in PIN1 localization in cells distal to the new convergence point and a reduction in the expression of PIN1 in cells above the convergence point (Fig. 8). In *unh-1,* the shift in PIN1 localization within the margin seems to occur normally, but the reduction in PIN1 expression fails to occur completely, resulting in an expanded MEPED. Although the apical-to-basal shift is believed to be controlled by *CUC2* (Bilsborough et al., 2011; Kawamura et al., 2010), the mechanism controlling PIN1 protein abundance within the marginal cells is not well understood. Mutations in *VTI11* and *VAM3*, which are localized to the PVC and vacuole, result in failure to target PIN1-GFP to the vacuole and in expanded MEPEDs (Shirakawa et al., 2009), suggesting that vacuolar targeting may play a role.

We propose that, like the GARP complex in other eukaryotes, UNH and the GARP complex play a key role in targeting proteins for degradation. Consistent with this conserved role, we have shown that UNH is localized to the TGN and PVC compartments, and that in *unh-1* mutants, a vacuolar targeted fluorophore (AVFY-RFP) fails to be targeted to the vacuole and is instead secreted to the apoplast. Furthermore, we propose that the expanded marginal PED in *unh-1* leaves may result from a failure to target PIN1 proteins properly to the lytic vacuole within leaf margin cells. Treatment of *unh-1* with BFA results in abnormal PIN1-GFP-containing compartments, suggesting that PIN1 trafficking is abnormal in *unh-1*. The *unh-1* phenotype is suppressed by *pin1-1*, consistent with the idea that the phenotype is the result of ectopic PIN1. We suggest that in *unh-1* mutants, endocytosed PIN1 is recycled back to the PM, leading to an expanded MEPED. Double mutants of *unh-1 vam3-4* or *unh-1 vti11* result in a leaf vein pattern that is additive between the two single mutants, supporting the idea that they act in independent steps that target *PIN1* to the vacuole.

Expanded epidermal PIN leads to the *unh-1* phenotype

Leaves of *unh-1* have fewer secondary veins and form extra serrations, two characteristics that are proposed to be controlled by PIN1 convergence points in epidermal cells of the leaf margin (Bilsborough et al., 2011; Scarpella et al., 2006; Wabnik et al., 2010; Wenzel et al., 2007). In *unh-1* mutants, although the subcellular localization of PIN1-GFP in margin cells appears normal, each MEPED associated with newly forming secondary veins is expanded. Subsequently, within the secondary vein PED, the formation of the LLD appears normal, but the ULD often does not form completely (Figs 7, 8).

The simplest explanation for the *unh-1* leaf phenotype is that expanded MEPEDs directly result in more serrations and fewer meeting secondary veins. This idea is supported by the inverse

Development (2014) 141, 1894-1905 doi:10.1242/dev.099333

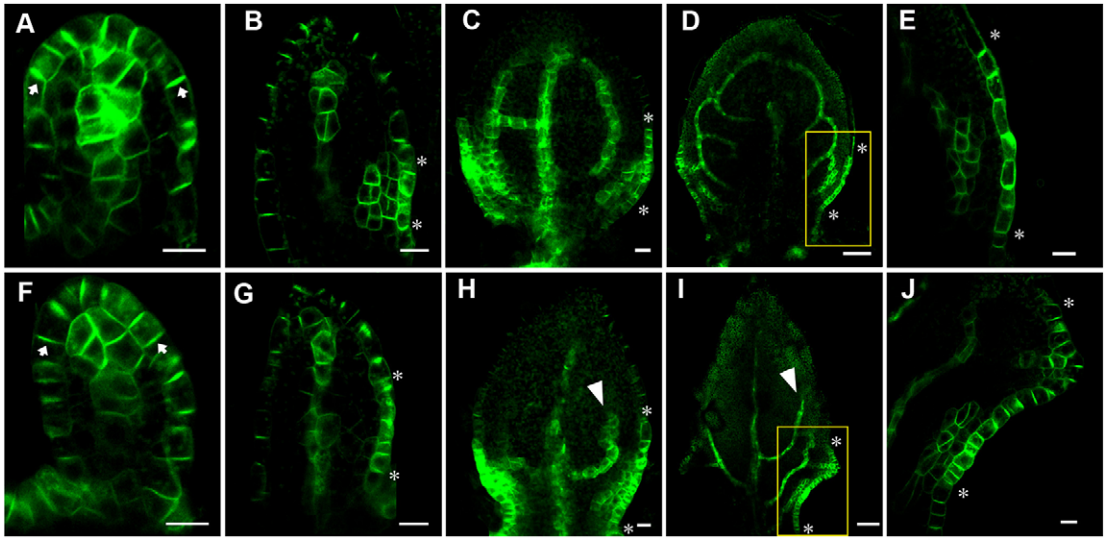

Fig. 7. PIN1-GFP expression in wild type and *unh-1*. First leaf primordia at 2 DAG (A), 2.5 DAG (B,F), 3 DAG (C,G), 4 DAG (D,E,H) and 5 DAG (I,J). (E,J) Enlargements of the boxed areas in D,I, respectively. Arrows in A and F represent the apical localization of PIN1-GFP in epidermis. Arrowheads in H and I represent the termination of the LLD in *unh-1* secondary veins. PIN1-GFP expression within the epidermis at the lateral margin (lateral PED) is flanked by asterisks. Viewed with confocal microscopy. Scale bars: 10 μm in A-C,E-G,H,J; 50 μm in D,I.

correlation between number of serrations and meeting secondary veins in double mutants between *unh-1* and mutations known to affect marginal PIN1 expression. Distal non-meeting of *unh-1* secondary veins is partially suppressed by *pin1-1* and *cuc2-3*, leading to the conclusion that the lack of meeting and failure to form a ULD is the indirect result of excess PIN1 in the margin. The reduction in tertiary and quaternary veins associated with *unh-1* is suppressed by *pin1-1*, but not by *cuc2-3*, suggesting that this defect is not associated with expansion of the MEPED and that *unh-1* may also affect PIN1 within developing veins of the lamina.

We speculate that the expanded MEPED results in a greater marginal auxin source that induces more margin outgrowth and alters auxin flux through the LLD (compare LLD in Fig. 8B and 8E), as indicated by reduced DR5:GUS expression in *unh-1* leaf veins. Consistent with the telome theory of leaf evolution (Beerling and Fleming, 2007), we suggest that epidermal auxin sources at the distal tip and lateral convergence points compete in much the same way as the SAM competes with a lateral meristem during lateral bud outgrowth (Prusinkiewicz et al., 2009; Wabnik et al., 2010) with flux through the midvein analogous to flux from the apical meristem, and flux from the MEPEDs through the secondary veins analogous to flux from the lateral buds. We suggest that, as in lateral buds (Prusinkiewicz et al., 2009), achieving a crucial level of auxin flux in successive secondary veins is required to allow auxin flux through the ULD. In *unh-1* mutants, the marginal source is expanded, auxin flux through the LLD is changed and the ULD fails to form (compare Fig. 8C with 8F).

MATERIALS AND METHODS

Plant materials and growth conditions

Arabidopsis thaliana, Columbia (Col-O) ecotype, was used as a wild-type control in all experiments and as a background for all the mutants, except *pin1-1* (Enkheim ecotype). Ethyl methane sulfonate-treated lines of *Arabidopsis* were obtained from Lehle Seed (Round Rock, TX, USA). *pin1-1,* DR5:GUS, *vam3-4*, *cuc2-3*, *BDLbdl* and *vti11* seed were from Thomas Berleth (University of Toronto, ON, Canada), Jane Murfett (University of Missouri-Columbia, MO, USA), Taku Takahashi (Ohtomo et al., 2005), Mitsuhiro Aida (Nara Institute of Science and Technology, Ikoma, Japan), Enrico Scarpella (University of Alberta, AB, Canada) and Miyo Morita (Kato et al., 2002), respectively. The PIN1-GFP, ATHB8:GUS and Salk T-DNA insertion lines were from the Arabidopsis Biological Resource Centre (ABRC, OH, USA). The T-DNA insertion line GABI_520G08 was from GABI-kat (Kleinboelting et al., 2012). Vectors pGreen229 (Hellens et al., 2000) and pBI:GUS (pBI101.2) were from Shelly Hepworth (Carleton University, ON, Canada), SYP61-YFP was from Luciana Renna (Stefano et al., 2010), pVKH18-GFPN was from Hugo Zheng (McGill University, QC, Canada) and WAVE constructs were from ABRC. *Arabidopis* (Steynen and Schultz, 2003) and *Nicotiana tabacum* SR1 (cv Petit Havana) (Brandizzi et al., 2002) were grown as described previously. The day of transfer of plants to growth chamber is referred to as 0 days after germination (DAG).

Table 3. PIN1:GFP expression in early leaf veins and margins

Genotype and stage	Number of secondary vein PEDs	Number of tertiary vein PEDs	Number of cells in marginal PEDs	Primordium length (μm)
Wild type 2.5 DAG	0.7±0.4 (23)	0 (23)	3.9±0.9 (15)	108.8±9.4 (23)
Wild type 3 DAG	3.2±1.6 (20)	0.7±1.3 (20)	6.3±1.5 (42)	144.5±23.0 (30)
Wild type 4 DAG	5.9±1.5 (20)	1.8±1.4 (20)	7.04±3.0 (67)	352.7±75.7 (15)
Wild type 5 DAG	ND	ND	6.0±1.6 (16)	490.8±63.2 (16)
unh-1 3 DAG	0.9±1.1 (37)*	0 (37)	6.8±1.4 (39)‡	114.4±17.2 (25)*
unh-1 4 DAG	2.4±0.8 (21)*	0 (21)*‡	9.2±3.3 (49)*‡	185.8±19.9 (15)*‡
unh-1 5 DAG	3.5±0.8 (14)‡	0.1±0.5 (14)‡	12.8±3.8 (38)*‡	438.1±49.5 (15)*‡

Values represent mean±s.d. Number in parentheses represents sample size. Distinct PIN1:GFP expression was rarely visible in distal secondary veins and tertiary veins in wild-type 5 DAG first leaves.

PED, PIN1:GFP expression domain (showing strong lateral expression – see supplementary material Fig. S6 for details); ND, not determined.

*Significantly different from wild type at the same day after germination (Student's *t*-test, $P<0.05$).

‡Significantly different from wild type at the same stage of development (Student's *t*-test, $P<0.05$).

Development (2014) 141, 1894-1905 doi:10.1242/dev.099333

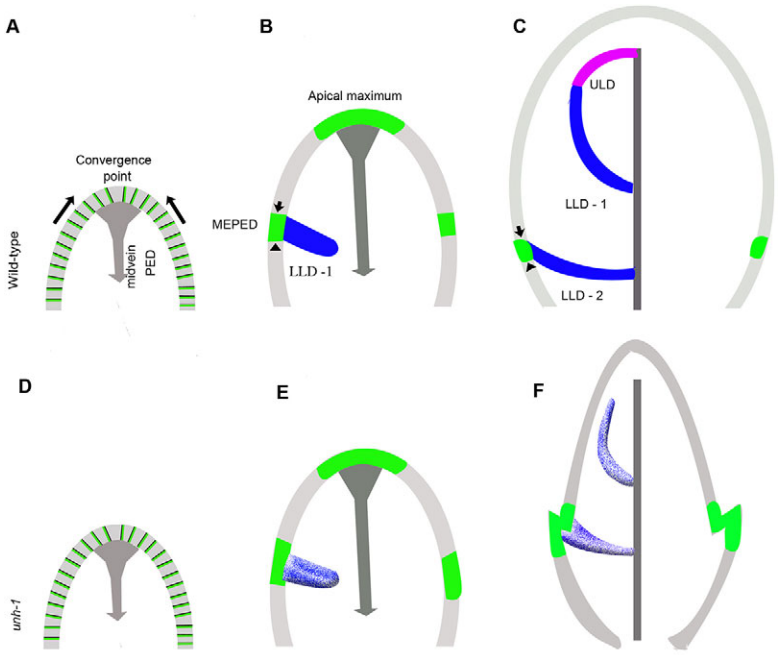

Fig. 8. Model for the role of marginal epidermal PIN1 expression domains in leaf vein patterning. (A) At early stages in wild type, PIN1 is localized apically (green) on all epidermal cells, generating a convergence point towards the apex (arrows). (B) The convergence point establishes an auxin maximum that generates the midvein PIN1 expression domain (PED). A switch in PIN1 polarity, together with reduced PIN1 levels, positions lateral marginal epidermal PED (MEPED) that initiate LLD for the first set of secondary veins (LLD-1). (C) LLD-1 is extended and the PED is completed distally by the upper loop domain (ULD) (magenta). The MEPEDs shift proximally and LLD-2 is initiated. (D) In *unh-1*, the establishment of the distal convergence point and the midvein occurs normally. (E) Reduced PIN1 targeting to the lytic vacuole results in expansion of the MEPED (green), which is associated with the first LLD and results in altered auxin flux (stippling of LLD) compared with wild type. (F) Differential flux of auxin through LLD-1 prevents auxin flux through the ULD.

Identification and mapping of *unh-1*

The *unh-1* mutant was backcrossed to wild type at least four times prior to all analyses. The location of *unh-1* mutation was narrowed down to 15 candidate protein-coding genes on chromosome 4, through segregation of polymorphisms identified through the Cereon polymorphism database (supplementary material Table S1) (Jander et al., 2002) in the F2 population (n=230) of an *unh-1* (Col-0) by Landsberg *erecta* (L*er*) cross. Sequencing of the candidate genes revealed a mutation in At4g02030. Genotyping of GABI_520G08 (*unh-2*) was performed by PCR using the primer set UNH_GABI_genespecific and UNH_GABI_PCR (supplementary material Table S2). Plants homozygous for GABI_520G08 were crossed to *unh-1* and allelism was confirmed by non-complementation in F1 plants.

Constructs and transformation

All primers used in amplification are listed in supplementary material Table S2. To generate the complementation construct (pUNH), 10 kb of wild-type genomic sequence, including 5000 bp upstream from the putative At4g02030 translation start site and 425 bp downstream from the putative translation termination site, was amplified from wild-type genomic DNA and ligated into the *Not*I sites of the pG229 II binary vector (Hellens et al., 2000). For generating a transcriptional fusion of the *UNH* transcriptional regulatory region to the GUS reporter gene (UNH_{prom}:GUS), the 5 kb upstream region was amplified and subcloned into the *Xma*I-cloning site 5′ to the B-Glucoronidase/*uidA* (*GUS*) reporter gene within the pBI:GUS binary vector. To generate the 35S:UNH-GFP construct, UNH cDNA was amplified from RAFL16-14-018 (pda19438, Riken BioResource Centre, Japan) and ligated into the *Sal*I sites of the pVKH18-GFPN binary vector, such that GFP is N-terminal to UNH. Plants homozygous for the *unh-1* mutation were transformed with pUNH and UNH-GFP, and wild-type plants were transformed with UNH_{prom}:GUS using the floral spray method (Hooker et al., 2007). T1 transformants were identified by resistance to BASTA on soil for pUNH or UNH-GFP, and to 25 µM kanamycin on plates for UNH_{prom}:GUS. Multiple T2 lines of UNH_{prom}:GUS showing 100% resistance to selection markers were screened and a representative T3 line was used for analysis. To generate the YPT6-YFP fusion, the pUNI vector (U83480) containing YPT6 cDNA was recombined with pNIGEL07 (Geldner et al., 2009).

For transient expression in tobacco, 35S:UNH-GFP, 35S:SYP61-YFP, YPT6-YFP, Wave 2_Y, Wave7_Y and Wave127_Y (Geldner et al., 2009) constructs were electroporated into *Agrobacterium tumefaciens* strain GV3101. As described previously (Batoko et al., 2000), bacterial cultures were pelleted, washed and resuspended in infiltration buffer to an OD600 value of 0.05 before being delivered into the abaxial epidermis of young tobacco leaves.

Transgenic lines and generation of double mutants

DR5:GUS (Ulmasov et al., 1997), ATHB8:GUS (Baima et al., 1995), 35S:AFVY-RFP (Hunter et al., 2007), 35S:EYFP-RABF2A (Preuss et al., 2004) and 35S:VAC-YFP (Nelson et al., 2007) were introduced into the *unh-1* background by crossing homozygous *unh-1* plants to each marker line. Homozygous F4 generation plants were used for analysis.

Double mutants were generated between *unh-1* and *pin1-1*, *vam3-4*, *vti11*, *cuc2-3* or *bdl*. With the exception of populations segregating for *pin1-1* and *bdl*, F3 lines with *unh-1* phenotype and showing segregation of the double mutant were allowed to self, and double mutant F4 plants were characterized. Homozygosity of *vam3-4*, *vti11* and *unh-1* was confirmed using mutation specific primers (Shirakawa et al., 2009). For *pin1-1* and *bdl*, plants with *unh-1* phenotype in the F2 were screened for the *pin1-1* allele [dCAPS primers: pin1-1dF and pin1-1R (v)] or for *BDL/bdl* based on epinastic leaves. Double mutants segregating in the F3 population were used for characterization.

RT-PCR

RNA was extracted from 100 mg of ground tissue using TRIzol reagent (Invitrogen) following the manufacturer's protocol. First-strand cDNA was generated from 1 µg total RNA using oligo(dT) primers and a RevertAid synthesis kit (Fermentas), and amplified using the UNHRTPCR_F and UNHRTPCR_R primer pair (supplementary material Table S2) flanking the *unh-1* and *unh-2* mutations. The protein phosphatase 2AA3 (At1g13320) (Czechowski et al., 2005) amplified with primer pair PP2A_F and PP2A_R (supplementary material Table S2) was used as a control.

GUS staining, phenotypic analysis and microscopy

GUS staining, cotyledon and leaf clearing, and analysis of vein phenotypes was performed as described previously (Kang and Dengler, 2002; Steynen and Schultz, 2003). In plants mutant for *pin1-1*, leaf fusion occurs with some frequency (3% of first leaves in both *unh-1* and *unh-1 pin1-1*, n=33 and 58, respectively). Because fused leaves merge leaves of two developmental stages (e.g. first and second leaves), they cannot be compared with either first or second leaves. Thus, we did not include them in our analysis of vein pattern and leaf shape. Where bifurcating midveins occurred in *unh-1 pin1-1* leaves (2%, n=56), the vein in the middle of the leaf was considered the midvein, whereas that angling to the margin was considered to be a secondary vein. Primary root length and root hairs were measured on 6 DAG seedlings grown vertically. Gravitropic response was measured 3 h after subjecting 4 DAG vertically grown roots to 90° rotation. All root measurements were carried out using NIH ImageJ software. Statistical differences were resolved using

Development (2014) 141, 1894-1905 doi:10.1242/dev.099333

ANOVA followed by Tukey-Kramer tests [leaf vein pattern, R project 3.0 (R Development Core Team, 2008)] or Student's *t*-test (all other analyses). Localization in *Arabidopsis* was performed and analyzed by confocal microscopy as described previously (Hou et al., 2010). For treatment with Brefeldin A (BFA) or Wortmannin, 4 DAG seedlings were placed in 50 µM BFA or 33 µM Wortmannin for 1.5 h and viewed immediately. For FM4-64, seedlings were placed in 8.2 µM FM4-64 for 30 min, rinsed in water and viewed after a further 30 min or 2.5 h. Transient expression in *N. tobaccum* leaves was analyzed 48 h after infection of the lower epidermis. An upright Leica SP5 or a FV1000 Olympus laser scanning confocal microscope was used to image the expression pattern (Brandizzi et al., 2002). All comparative analyses were carried out using images taken at the same microscope settings. Co-localization was determined by counting frequency of signal overlap in the merged images of at least 10 cells. In BFA, FM4-65 and Wortmannin-treated roots, cellular structure was analyzed in at least five cells in 10 roots; in cotyledons, structures expressing 35S:EYFP-RABF2A and 35S:VAC-YFP were quantified in a 70×70 µm area in 10 images. For comparison of PIN1-GFP levels, the coloration threshold was set to the same level of pixel density (supplementary material Fig. S7).

Yeast two-hybrid assay

A yeast two-hybrid screen was performed using a GAL4-based yeast two-hybrid system (Kohalmi et al., 1997). Full-length coding sequences for *UNH* (pda19438), *VPS52* (pda01753), *VPS53* (pda19355) and *VPS54* (pda08404) were obtained from RIKEN. Primer sets, labeled according to the gene name (supplementary material Table S2) were used to amplify *UNH*, *VPS52*, *VPS53* and *VPS54*. The amplified product was first ligated into Clonejet blunt (Fermentas) and then into the bait and prey vectors. *UNH* was ligated into the bait vector (pBI770) that expresses GAL4-DNA-binding (DB) fusion protein. The other coding sequences were ligated into the prey vector (pBI771) that expresses GAL4-transcription activation (TA) fusion protein. Yeast transformation and tests for self-activation and interaction were carried out as described previously (Garrett et al., 2012), with interacter (T4) and non-interacter (T7) of *AGAMOUS LIKE4* (*AGL4*) as positive and negative controls, respectively (Kohalmi et al., 1998).

Accession numbers

Sequence data for DNA and protein used in the study can be found in supplementary material Table S3.

Acknowledgements

We thank our colleagues who kindly donated seed and vectors, Douglas Bray for technical assistance in confocal microscopy, Rodrigo Ortego Polo for help with statistical analyses, and Federica Brandizzi and members of the Brandizzi lab for helpful discussions and assistance.

Competing interests

The authors declare no competing financial interests.

Author contributions

S.P., R.D.C. and E.A.S. developed concepts, performed experiments and data analysis, and prepared and edited manuscript; M.T.B., J.L.E. and C.L. performed experiments.

Funding

This work was funded by a Discovery Grant to E.A.S., by post-graduate scholarships to J.L.E. and by undergraduate summer research awards to M.T.B. (all from the Natural Science and Engineering Research Council, Canada).

Supplementary material

Supplementary material available online at
http://dev.biologists.org/lookup/suppl/doi:10.1242/dev.099333/-/DC1

References

Baima, S., Nobili, F., Sessa, G., Lucchetti, S., Ruberti, I. and Morelli, G. (1995). The expression of the Athb-8 homeobox gene is restricted to provascular cells in Arabidopsis thaliana. *Development* **121**, 4171-4182.

Batoko, H., Zheng, H. Q., Hawes, C. and Moore, I. (2000). A rab1 GTPase is required for transport between the endoplasmic reticulum and golgi apparatus and for normal golgi movement in plants. *Plant Cell* **12**, 2201-2218.

Bayer, E. M., Smith, R. S., Mandel, T., Nakayama, N., Sauer, M., Prusinkiewicz, P. and Kuhlemeier, C. (2009). Integration of transport-based models for phyllotaxis and midvein formation. *Genes Dev.* **23**, 373-384.

Beerling, D. J. and Fleming, A. J. (2007). Zimmermann's telome theory of megaphyll leaf evolution: a molecular and cellular critique. *Curr. Opin. Plant Biol.* **10**, 4-12.

Benková, E., Michniewicz, M., Sauer, M., Teichmann, T., Seifertová, D., Jürgens, G. and Friml, J. (2003). Local, efflux-dependent auxin gradients as a common module for plant organ formation. *Cell* **115**, 591-602.

Berleth, T. and Mattsson, J. (2000). Vascular development: tracing signals along veins. *Curr. Opin. Plant Biol.* **3**, 406-411.

Berleth, T., Mattsson, J. and Hardtke, C. S. (2000). Vascular continuity and auxin signals. *Trends Plant Sci.* **5**, 387-393.

Bilsborough, G. D., Runions, A., Barkoulas, M., Jenkins, H. W., Hasson, A., Galinha, C., Laufs, P., Hay, A., Prusinkiewicz, P. and Tsiantis, M. (2011). Model for the regulation of Arabidopsis thaliana leaf margin development. *Proc. Natl. Acad. Sci. U.S.A.* **108**, 3424-3429.

Bolte, S., Talbot, C., Boutte, Y., Catrice, O., Read, N. D. and Satiat-Jeunemaitre, B. (2004). FM-dyes as experimental probes for dissecting vesicle trafficking in living plant cells. *J. Microsc.* **214**, 159-173.

Brandizzi, F., Snapp, E. L., Roberts, A. G., Lippincott-Schwartz, J. and Hawes, C. (2002). Membrane protein transport between the endoplasmic reticulum and the Golgi in tobacco leaves is energy dependent but cytoskeleton independent: evidence from selective photobleaching. *Plant Cell* **14**, 1293-1309.

Conibear, E., Cleck, J. N. and Stevens, T. H. (2003). Vps51p mediates the association of the GARP (Vps52/53/54) complex with the late Golgi t-SNARE Tlg1p. *Mol. Biol. Cell* **14**, 1610-1623.

Czechowski, T., Stitt, M., Altmann, T., Udvardi, M. K. and Scheible, W. R. (2005). Genome-wide identification and testing of superior reference genes for transcript normalization in Arabidopsis. *Plant Physiol.* **139**, 5-17.

Dettmer, J., Hong-Hermesdorf, A., Stierhof, Y. D. and Schumacher, K. (2006). Vacuolar H+-ATPase activity is required for endocytic and secretory trafficking in Arabidopsis. *Plant Cell* **18**, 715-730.

Dhonukshe, P., Aniento, F., Hwang, I., Robinson, D. G., Mravec, J., Stierhof, Y.-D. and Friml, J. (2007). Clathrin-mediated constitutive endocytosis of PIN auxin efflux carriers in Arabidopsis. *Curr. Biol.* **17**, 520-527.

Ebine, K., Fujimoto, M., Okatani, Y., Nishiyama, T., Goh, T., Ito, E., Dainobu, T., Nishitani, A., Uemura, T., Sato, M. H. et al. (2011). A membrane trafficking pathway regulated by the plant-specific RAB GTPase ARA6. *Nat. Cell Biol.* **13**, 853-859.

Feraru, E., Paciorek, T., Feraru, M. I., Zwiewka, M., De Groodt, R., De Rycke, R., Kleine-Vehn, J. and Friml, J. (2010). The AP-3 beta adaptin mediates the biogenesis and function of lytic vacuoles in Arabidopsis. *Plant Cell* **22**, 2812-2824.

Garrett, J. J. T., Meents, M. J., Blackshaw, M. T., Blackshaw, L. C., Hou, H., Styranko, D. M., Kohalmi, S. E. and Schultz, E. A. (2012). A novel, semi-dominant allele of MONOPTEROS provides insight into leaf initiation and vein pattern formation. *Planta* **236**, 297-312.

Geldner, N., Anders, N., Wolters, H., Keicher, J., Kornberger, W., Muller, P., Delbarre, A., Ueda, T., Nakano, A. and Jürgens, G. (2003). The Arabidopsis GNOM ARF-GEF mediates endosomal recycling, auxin transport, and auxin-dependent plant growth. *Cell* **112**, 219-230.

Geldner, N., Dénervaud-Tendon, V., Hyman, D. L., Mayer, U., Stierhof, Y.-D. and Chory, J. (2009). Rapid, combinatorial analysis of membrane compartments in intact plants with a multicolor marker set. *Plant J.* **59**, 169-178.

Guermonprez, H., Smertenko, A., Crosnier, M.-T., Durandet, M., Vrielynck, N., Guerche, P., Hussey, P. J., Satiat-Jeunemaitre, B. and Bonhomme, S. (2008). The POK/AtVPS52 protein localizes to several distinct post-Golgi compartments in sporophytic and gametophytic cells. *J. Exp. Bot.* **59**, 3087-3098.

Hellens, R. P., Edwards, E. A., Leyland, N. R., Bean, S. and Mullineaux, P. M. (2000). pGreen: a versatile and flexible binary Ti vector for Agrobacterium-mediated plant transformation. *Plant Mol. Biol.* **42**, 819-832.

Hooker, T. S., Lam, P., Zheng, H. and Kunst, L. (2007). A core subunit of the RNA-processing/degrading exosome specifically influences cuticular wax biosynthesis in Arabidopsis. *Plant Cell* **19**, 904-913.

Hou, H., Erickson, J., Meservy, J. and Schultz, E. A. (2010). FORKED1 encodes a PH domain protein that is required for PIN1 localization in developing leaf veins. *Plant J.* **63**, 960-973.

Hunter, P. R., Craddock, C. P., Di Benedetto, S., Roberts, L. M. and Frigerio, L. (2007). Fluorescent reporter proteins for the tonoplast and the vacuolar lumen identify a single vacuolar compartment in Arabidopsis cells. *Plant Physiol.* **145**, 1371-1382.

Jander, G., Norris, S. R., Rounsley, S. D., Bush, D. F., Levin, I. M. and Last, R. L. (2002). Arabidopsis map-based cloning in the post-genome era. *Plant Physiol.* **129**, 440-450.

Johansen, J. N., Chow, C.-M., Moore, I. and Hawes, C. (2009). AtRAB-H1b and AtRAB-H1c GTPases, homologues of the yeast Ypt6, target reporter proteins to the Golgi when expressed in Nicotiana tabacum and Arabidopsis thaliana. *J. Exp. Bot.* **60**, 3179-3193.

Kang, J. and Dengler, N. (2002). Cell cycling frequency and expression of the homeobox gene ATHB-8 during leaf vein development in Arabidopsis. *Planta* **216**, 212-219.
Kato, T., Morita, M. T., Fukaki, H., Yamauchi, Y., Uehara, M., Niihama, M. and Tasaka, M. (2002). SGR2, a phospholipase-like protein, and ZIG/SGR4, a SNARE, are involved in the shoot gravitropism of Arabidopsis. *Plant Cell* **14**, 33-46.
Kawamura, E., Horiguchi, G. and Tsukaya, H. (2010). Mechanisms of leaf tooth formation in Arabidopsis. *Plant J.* **62**, 429-441.
Kleinboelting, N., Huep, G., Kloetgen, A., Viehoever, P. and Weisshaar, B. (2012). GABI-Kat SimpleSearch: new features of the Arabidopsis thaliana T-DNA mutant database. *Nucleic Acids Res.* **40**, D1211-D1215.
Kleine-Vehn, J., Leitner, J., Zwiewka, M., Sauer, M., Abas, L., Luschnig, C. and Friml, J. (2008). Differential degradation of PIN2 auxin efflux carrier by retromer-dependent vacuolar targeting. *Proc. Natl. Acad. Sci. U.S.A.* **105**, 17812-17817.
Kohalmi, S. E., Nowak, J. and Crosby, W. L. (1997). A practical guide to using the yeast 2-hybrid system. In *Differentially Expressed Genes in Plants: A Bench Manual* (ed. E. Hansen and G. Harper), pp. 63-82. London: Taylor and Francis.
Kohalmi, S. E., Reader, L. J. V., Samach, A., Nowak, J., Haughn, G. W. and Crosby, W. L. (1998). Identification and characterization of protein interactions using the yeast 2-hybrid system. In Plant Molecular Biology Manual (ed. S. B. Gelvin and R. A. Schiperoort), pp. 1-30. The Netherlands: Kluwer Academic Publishers.
Koizumi, K., Naramoto, S., Sawa, S., Yahara, N., Ueda, T., Nakano, A., Sugiyama, M. and Fukuda, H. (2005). VAN3 ARF-GAP-mediated vesicle transport is involved in leaf vascular network formation. *Development* **132**, 1699-1711.
Koumandou, V. L., Dacks, J. B., Coulson, R. M. R. and Field, M. C. (2007). Control systems for membrane fusion in the ancestral eukaryote; evolution of tethering complexes and SM proteins. *BMC Evol. Biol.* **7**, 29.
Laxmi, A., Pan, J., Morsy, M. and Chen, R. (2008). Light plays an essential role in intracellular distribution of auxin efflux carrier PIN2 in Arabidopsis thaliana. *PLoS ONE* **3**, e1510.
Lee, G.-J., Sohn, E. J., Lee, M. H. and Hwang, I. (2004). The Arabidopsis Rab5 homologs Rha1 and Ara7 localize to the prevacuolar compartment. *Plant Cell Physiol.* **45**, 1211-1220.
Lee, C.-F., Pu, H.-Y., Wang, L.-C., Sayler, R. J., Yeh, C.-H. and Wu, S.-J. (2006). Mutation in a homolog of yeast Vps53p accounts for the heat and osmotic hypersensitive phenotypes in Arabidopsis hit1-1 mutant. *Planta* **224**, 330-338.
Lobstein, E., Guyon, A., Férault, M., Twell, D., Pelletier, G. and Bonhomme, S. (2004). The putative Arabidopsis homolog of yeast vps52p is required for pollen tube elongation, localizes to Golgi, and might be involved in vesicle trafficking. *Plant Physiol.* **135**, 1480-1490.
Luo, L., Hannemann, M., Koenig, S., Hegermann, J., Ailion, M., Cho, M.-K., Sasidharan, N., Zweckstetter, M., Rensing, S. A. and Eimer, S. (2011). The Caenorhabditis elegans GARP complex contains the conserved Vps51 subunit and is required to maintain lysosomal morphology. *Mol. Biol. Cell* **22**, 2564-2578.
Marchler-Bauer, A., Lu, S., Anderson, J. B., Chitsaz, F., Derbyshire, M. K., DeWeese-Scott, C., Fong, J. H., Geer, L. Y., Geer, R. C., Gonzales, N. R. et al. (2011). CDD: a Conserved Domain Database for the functional annotation of proteins. *Nucleic Acids Res.* **39**, D225-D229.
Nelson, B. K., Cai, X. and Nebenführ, A. (2007). A multicolored set of in vivo organelle markers for co-localization studies in Arabidopsis and other plants. *Plant J.* **51**, 1126-1136.
Ohtomo, I., Ueda, H., Shimada, T., Nishiyama, C., Komoto, Y., Hara-Nishimura, I. and Takahashi, T. (2005). Identification of an allele of VAM3/SYP22 that confers a semi-dwarf phenotype in Arabidopsis thaliana. *Plant Cell Physiol.* **46**, 1358-1365.
Oliviusson, P., Heinzerling, O., Hillmer, S., Hinz, G., Tse, Y. C., Jiang, L. and Robinson, D. G. (2006). Plant retromer, localized to the prevacuolar compartment and microvesicles in Arabidopsis, may interact with vacuolar sorting receptors. *Plant Cell* **18**, 1239-1252.
Perez-Victoria, F. J. and Bonifacino, J. S. (2009). Dual roles of the mammalian GARP complex in tethering and SNARE complex assembly at the trans-golgi network. *Mol. Cell. Biol.* **29**, 5251-5263.
Perez-Victoria, F. J., Mardones, G. A. and Bonifacino, J. S. (2008). Requirement of the human GARP complex for mannose 6-phosphate-receptor-dependent sorting of cathepsin D to lysosomes. *Mol. Biol. Cell* **19**, 2350-2362.
Perez-Victoria, F. J., Abascal-Palacios, G., Tascon, I., Kajava, A., Magadan, J. G., Pioro, E. P., Bonifacino, J. S. and Hierro, A. (2010a). Structural basis for the wobbler mouse neurodegenerative disorder caused by mutation in the Vps54 subunit of the GARP complex. *Proc. Natl. Acad. Sci. U.S.A.* **107**, 12860-12865.
Perez-Victoria, F. J., Schindler, C., Magadan, J. G., Mardones, G. A., Delevoye, C., Romao, M., Raposo, G. and Bonifacino, J. S. (2010b). Ang2/fat-free is a conserved subunit of the Golgi-associated retrograde protein complex. *Mol. Biol. Cell* **21**, 3386-3395.
Preuss, M. L., Serna, J., Falbel, T. G., Bednarek, S. Y. and Nielsen, E. (2004). The Arabidopsis Rab GTPase RabA4b localizes to the tips of growing root hair cells. *Plant Cell* **16**, 1589-1603.
Prusinkiewicz, P., Crawford, S., Smith, R. S., Ljung, K., Bennett, T., Ongaro, V. and Leyser, O. (2009). Control of bud activation by an auxin transport switch. *Proc. Natl. Acad. Sci. U.S.A.* **106**, 17431-17436.
Quint, M. and Gray, W. M. (2006). Auxin signaling. *Curr. Opin. Plant Biol.* **9**, 448-453.
R Development Core Team (2008). *R: A Language and Environment for Statistical Computing*. Vienna, Austria: R Foundation for Statistical Computing. ISBN 3-900051-07-0. http://www.R-project.org
Reggiori, F., Wang, C. W., Stromhaug, P. E., Shintani, T. and Klionsky, D. J. (2003). Vps51 is part of the yeast Vps fifty-three tethering complex essential for retrograde traffic from the early endosome and Cvt vesicle completion. *J. Biol. Chem.* **278**, 5009-5020.
Reinhardt, D., Pesce, E.-R., Stieger, P., Mandel, T., Baltensperger, K., Bennett, M., Traas, J., Friml, J. and Kuhlemeier, C. (2003). Regulation of phyllotaxis by polar auxin transport. *Nature* **426**, 255-260.
Sachs, T. (1981). The control of the patterned differentiation of vascular tissues. *Adv. Bot. Res.* **9**, 151-262.
Saito, C., Ueda, T., Abe, H., Wada, Y., Kuroiwa, T., Hisada, A., Furuya, M. and Nakano, A. (2002). A complex and mobile structure forms a distinct subregion within the continuous vacuolar membrane in young cotyledons of Arabidopsis. *Plant J.* **29**, 245-255.
Sanderfoot, A. A., Kovaleva, V., Bassham, D. C. and Raikhel, N. V. (2001). Interactions between syntaxins identify at least five SNARE complexes within the Golgi/prevacuolar system of the Arabidopsis cell. *Mol. Biol. Cell* **12**, 3733-3743.
Scarpella, E., Francis, P. and Berleth, T. (2004). Stage-specific markers define early steps of procambium development in Arabidopsis leaves and correlate termination of vein formation with mesophyll differentiation. *Development* **131**, 3445-3455.
Scarpella, E., Marcos, D., Friml, J. and Berleth, T. (2006). Control of leaf vascular patterning by polar auxin transport. *Genes Dev.* **20**, 1015-1027.
Scarpella, E., Barkoulas, M. and Tsiantis, M. (2010). Control of leaf and vein development by auxin. *Cold Spring Harb. Perspect. Biol.* **2**, a001511.
Schmitt-John, T., Drepper, C., Mussmann, A., Hahn, P., Kuhlmann, M., Thiel, C., Hafner, M., Lengeling, A., Heimann, P., Jones, J. M. et al. (2005). Mutation of Vps54 causes motor neuron disease and defective spermiogenesis in the wobbler mouse. *Nat. Genet.* **37**, 1213-1215.
Shirakawa, M., Ueda, H., Shimada, T., Nishiyama, C. and Hara-Nishimura, I. (2009). Vacuolar SNAREs function in the formation of the leaf vascular network by regulating auxin distribution. *Plant Cell Physiol.* **50**, 1319-1328.
Siniossoglou, S. and Pelham, H. R. (2002). Vps51p links the VFT complex to the SNARE Tlg1p. *J. Biol. Chem.* **277**, 48318-48324.
Spitzer, C., Reyes, F. C., Buono, R., Sliwinski, M. K., Haas, T. J. and Otegui, M. S. (2009). The ESCRT-related CHMP1A and B proteins mediate multivesicular body sorting of auxin carriers in Arabidopsis and are required for plant development. *Plant Cell* **21**, 749-766.
Stefano, G., Renna, L., Rossi, M., Azzarello, E., Pollastri, S., Brandizzi, F., Baluska, F. and Mancuso, S. (2010). AGD5 is a GTPase-activating protein at the trans-Golgi network. *Plant J.* **64**, 790-799.
Steinmann, T., Geldner, N., Grebe, M., Mangold, S., Jackson, C. L., Paris, S., Gälweiler, L., Palme, K. and Jürgens, G. (1999). Coordinated polar localization of auxin efflux carrier PIN1 by GNOM ARF GEF. *Science* **286**, 316-318.
Steynen, Q. J. and Schultz, E. A. (2003). The FORKED genes are essential for distal vein meeting in Arabidopsis. *Development* **130**, 4695-4708.
Uemura, T., Ueda, T., Ohniwa, R. L., Nakano, A., Takeyasu, K. and Sato, M. H. (2004). Systematic analysis of SNARE molecules in Arabidopsis: dissection of the post-Golgi network in plant cells. *Cell. Struct. Funct.* **29**, 49-65.
Ulmasov, T., Hagen, G. and Guilfoyle, T. J. (1997). ARF1, a transcription factor that binds to auxin response elements. *Science* **276**, 1865-1868.
Wabnik, K., Kleine-Vehn, J., Balla, J., Sauer, M., Naramoto, S., Reinöhl, V., Merks, R. M. H., Govaerts, W. and Friml, J. (2010). Emergence of tissue polarization from synergy of intracellular and extracellular auxin signaling. *Mol. Syst. Biol.* **6**, 447.
Wang, L.-C., Tsai, M.-C., Chang, K.-Y., Fan, Y.-S., Yeh, C.-H. and Wu, S.-J. (2011). Involvement of the Arabidopsis HIT1/AtVPS53 tethering protein homologue in the acclimation of the plasma membrane to heat stress. *J. Exp. Bot.* **62**, 3609-3620.
Wenzel, C. L., Schuetz, M., Yu, Q. and Mattsson, J. (2007). Dynamics of MONOPTEROS and PIN-FORMED1 expression during leaf vein pattern formation in Arabidopsis thaliana. *Plant J.* **49**, 387-398.